Journal of Applied Polymer Science

Nanoindentation Response of Poly(ether ether ketone) Surfaces—A Semicrystalline Bimodal Behavior

Tanveer Iqbal,[1] Brian J. Briscoe,[2] Saima Yasin,[2] Paul F. Luckham[2]

[1]Chemical Engineering Department, University of Engineering & Technology, KSK Campus, Lahore, Pakistan
[2]Chemical Engineering Department, Imperial College, South Kensington, London SW7 2AZ, United Kingdom
Correspondence to: T. Iqbal (E-mail: t.iqbal07@imperial.ac.uk or tanveer@uet.edu.pk)

ABSTRACT: Indentation is a relatively simple and virtually nondestructive technique of assessing mechanical properties of materials by an indenter inducing localized deformation into a solid surface. The load–displacement curves, the hardness, and the elastic modulus data together with associated analysis for poly(ether ether ketone) (PEEK) surfaces are presented as a function of contact displacement. The major conclusions are that nanoindentation into the polymer show a surface hardening response that is dependent upon the contact conditions. PEEK, a semicrystalline polymer, has bimodal nanoindentation characteristics because of the presence of hard crystalline lamella within a softer amorphous phase. The bimodal character is confirmed by the load–displacement, the hardness, and the elastic modulus data. The semicrystalline polymer exhibits periodic fluctuations in mechanical properties with the increasing penetration depth. Finally, the nanoindentation is found to be a convenient method to estimate the degree of crystallinity of semicrystalline polymers. The technique may provide a convenient means to understand morphological description of the polymeric surfaces.

KEYWORDS: surfaces and interfaces; properties and characterization; coatings; mechanical properties

Received 9 April 2013; accepted 30 June 2013; Published online 20 July 2013
DOI: 10.1002/app.39723

INTRODUCTION

The evaluation of material properties at the very first surface molecular layers has always been a challenge. It is believed that these properties govern some aspects of the contact performance of these materials especially in many surface engineering and tribological applications. Therefore, material selection and design for such applications profit from knowledge of near surface properties. Indentation at the nano scale has been established as a convenient method to investigate the mechanical properties of materials at reduced penetration depths for the past two decades.[1–11]

The near surface mechanical properties investigation by indentation is challenging. Any method that relies on optical imaging of the contact after indentation is not suitable because of large and unacceptable errors for small scale indentations. This problem has been largely overcome by the use of a contact compliance method based on the measurement of the reaction force on the indenter as a function of the imposed displacement, or vice versa, resulting in a set of loading and unloading curves for each indentation operation. The hardness and the elastic modulus are computed entirely from the analysis of the load–displacement curves obtained from the loading–unloading cycles performed. Therefore, measurement of the residual contact area is not required in this method.[12,13] The inevitable presence of imperfections in indenter tip geometry is another problem encountered during the hardness evaluation by indentation.[14,15] These tip defects could be comparable to the full indent size and might cause a significant error in the evaluated property values. Briscoe and Sebastian[2] have examined this problem for polymeric materials and proposed an analytical method based on tip defect estimation.

The response of polymeric materials during the unloading segment of the indentation experiment may show a creeping effect; that is, immediately after the unloading segment begins, the penetration depth slightly increases, although the imposed load decreases at a constant rate. This means that the material creeping rate is higher in magnitude than the imposed unloading rate during the first portion of the unloading; this effect may be encountered even at the highest available unloading rates. The creeping effect may be readily detected by the occurrence of a characteristically round shape of the data, "a nose", at the correspondence of the loading–unloading peak. This phenomenon, which may be anticipated in view of the highly time-dependent deformation and relaxation nature of polymers, may dramatically affect the evaluation of the hardness of these surfaces (no elastic or viscoelastic recovery seems to occur at the incipient

unloading). This problem can be avoided by providing a definite hold segment at the maximum load before subsequent unloading.[6,7]

The interpretation of the indentation of polymeric surfaces poses further difficulties because of the complex viscoelastic-plastic response of such materials as well as their thermal sensitivity. Polymers show different behaviors under different contact conditions because of strain and strain-rate dependence of their properties. Therefore, the surface mechanical properties of polymers are a function of the imposed contact conditions, such as the indenter geometry, the penetration depth (the strain), the loading rate (i.e. strain rate), and the ambient temperature. The overall mechanical properties of semicrystalline polymers are strongly influenced by the degree of crystallinity of the polymer.[16] The degree of crystallinity of a semicrystalline polymer can be varied to some limited degree by following different thermal treatments, for example quenching the melt produces an amorphous, whereas annealing produces a crystalline (semicrystalline) polymer.

PEEK, poly(oxy-1,4-phenylene-oxy-1,4-phenylenecarbonyl-1,4-phenylene), is a highly aromatic semicrystalline thermoplastic polymer, first commercially synthesized in 1975.[17] It may be manufactured in both amorphous and semicrystalline grades with the maximum achievable crystallinity of ca. 48%. PEEK has a specific gravity of 1.265 in the amorphous state and 1.320 with maximum achievable crystallinity. Typical values of molecular weight for the PEEK are 30,000–-45,000.[18] The semicrystalline PEEK samples were melted and then quenched (rapid cooling) in water, to produce the amorphous PEEK and annealed (slower or controlled cooling) to produce the crystalline polymer. The load–displacement curves, the hardness, and the elastic modulus data obtained from the nanoindentation and subsequent associated analysis for an amorphous and a semicrystalline PEEK surfaces are reported as a function of contact displacement.

EXPERIMENTAL

Nanoindenter

The normal indentation hardness experiments were conducted using a NANO INDENTER® IIs machine, supplied by Nano Instruments, TN, USA. A continuous contact compliance indentation mode has been adopted with the machine.[12] Therefore, the nanoindentation machine has the ability to enable the experimental determination of the indentation hardness and the elastic modulus of material being indented without actual measurement of the area of indentation. The machine is capable of operating in the microgram load range. The theoretical depth resolution of the indenter is in the nanometer range. A three sided diamond pyramid tip, a Berkovich Tip, is attached at the bottom of the indenter rod. The sides of the pyramid tip make an angle of 65.3° normal to the base. Therefore, perfectly plastic indents, using a Berkovich Tip, appear as equilateral triangles. An electromagnetic aluminium coil surrounded by a solenoid magnetic field connected at the top of inner indenter tube is utilized to apply the normal load. A three-plate capacitive displacement sensor measures displacement of the indenter tip.

The geometry of the diamond indenter tip and hence area of indentation was resolved by indenting against fused silica and performing the indent area calibrations using indenter area function presented in the following equation:

$$A = 24.5h_c^2 + m_1 h_c + m_2 h_c^{1/2} + m_3 h_c^{1/4} + m_4 h_c^{1/8} + m_5 h_c^{1/16} + m_6 h_c^{1/32} + m_7 h_c^{1/64} + m_8 h_c^{1/128} \quad (1)$$

where A is the area based on indentation displacement, h_c. The silica is presumed to be spatially homogenous mechanically. An initial factor of 24.5 is used to account for the perfect Berkovich tip indenter. The load frame stiffness of the nanoindenter was calculated to be 7.05×10^7 N/m and the tip area function coefficients to be used in indenter area function, equation 1 were

$m_1 = -2.55 \times 10^{-5}$, $m_2 = -6.45 \times 10^{-6}$, $m_3 = -1.71 \times 10^{-4}$,
$m_4 = -3.96 \times 10^{-5}$, $m_5 = 6.55 \times 10^{-5}$, $m_6 = -1.08 \times 10^{-4}$,
$m_7 = -2.12 \times 10^{-4}$, $m_8 = -3.36 \times 10^{-5}$

Hardness and elastic modulus were calculated as a continuous function of the penetration depth using the continuous stiffness indentation mode(NANO INDENTER® IIs, operating instructions).[19,20] The continuous stiffness method utilizes the superimposition of a very small AC current onto the DC current loading ramp system. As a result the probe tip oscillates at 1 nm amplitude at a frequency of 45 Hz during the indentation loading segment. Therefore, small compliance curves consisting of the loading and unloading from superposition were generated during the indentation loading process. Hence the material parameters such as the hardness and the modulus were deduced as a continuous function of indentation displacement. The continuous stiffness mode is particularly useful for polymeric materials because of the large variation in mechanical properties and the presence of the negative slope in the initial unloading segment because of creep.[6]

Materials

Commercially available semicrystalline PEEK 1.2-mm-thick sheets, Goodfellow catalogue # EK303031, Cambridge, UK, were used. The crystallinity of the virgin semicrystalline sample was estimated to be 40% by the differential scanning calorimeter (DSC).[21] The polymer samples were melted using a 3–mm-thick aluminium sheets on a hot press, at a temperature of 380–400°C, to produce crystalline and amorphous samples. The crystalline samples were produced by allowing the sample to cool gradually (annealing) to ambient temperature. The annealed samples were found to possess 31% crystalline content by DSC analysis. Whereas quenching the heated samples in cold water produced amorphous samples, which had negligible crystalline content. The average peak surface roughness of these samples was evaluated using an optical profilometer and ranged between 0.1 and 0.5 μm. The surface roughness which affects nanoindentation results is much smaller than those measured by conventional profilometry.

Procedure

Continuous stiffness nanoindentation experiments were conducted on virgin, quenched and annealed PEEK samples at constant loading rate of 300μN/sec to a maximum depth of 5000 nm. Constant effective strain rates (0.025 sec^{-1}) and constant

displacement rate (5 nm/sec) experiments were also performed on virgin PEEK samples. The effective constant strain rates were achieved by application of constant displacement rate segments for different indentation displacement. The indenter was held for 20 sec at the maximum load to account for the material creep behavior of the polymer surface. A final hold segment of 50 sec after 80% unloading was applied to account for the thermal drift during all indentation experiment. Hardness and elastic modulus were calculated as a continuous function of penetration depth using continuous stiffness indentation mode.[19,20] All polymeric samples were indented at 50 different locations nominally 100 μm apart.

RESULTS AND DISCUSSION

Load–Displacement Curves

Figures 1–3 present typical loading–unloading cycle data curves of the quenched (amorphous), the virgin (semicrystalline), and the annealed (semicrystalline) PEEK surfaces, respectively. The data were obtained at constant loading–unloading rates of 300 μN/sec upto a maximum penetration depth of 5000 nm. The indents were spaced ca., 100 μm from each other. The loading portion of an indentation cycle starts from 0 nm indentation displacement to a maximum displacement of 5000 nm at maximum load to account for material creep. The loading portion was followed by a hold segment (20 sec) at the maximum indentation load to account for the creeping effect. The unloading step starts from the maximum load to an unrecoverable indentation depth at zero load of the surface. A constant load hold step of 50 sec, after 80% unloading, was provided in the unloading segment at 80% load recovery to account for the thermal drift in the indentation experiments. The indentation reaction load was observed to remain near zero for all indentation experiments at low penetration depth (approximately <100 nm) during loading. This region is termed as the induction phase of the indentation experiment[22] and may have arisen from the surface determination errors, the unaccountable physical imperfections of the indenter tip and the uncertainties associated with the calibration procedures. The surface determination errors results from the surface roughness at nanometric scale of the surfaces. The precise range of the induction phase is inevitably unknown, therefore the load–displacement data are presented as that obtained from the machine. The indenter to the surface contact was established based on a doubling of the contact stiffness. A better insight can be gained from the subsequent data on the hardness and modulus. The tip area function and the contact stiffness of the indenter were calibrated against a fused silica, which has a 10^2 to 10^4times higher modulus than the polymeric surfaces, prior to indentation experiments on the polymers. The requirement of a standard material with Young's Modulus comparable to the polymeric surfaces, for the tip area calibrations and the stiffness, is anticipated in the future. An unsuccessful effort was made to calibrate the tip area function and the load frame stiffness against a polystyrene (PS) surface; the natural surface hardening of the PS was thought to be the major reason for this failure.

Figure 1 presents typical load–displacement data of the quenched (amorphous) PEEK samples. The loading curves from different indentations spaced ca. 100 μm apart performed on the quenched PEEK samples showed a fairly consistent response. The maximum indentation displacement of 5000 nm was

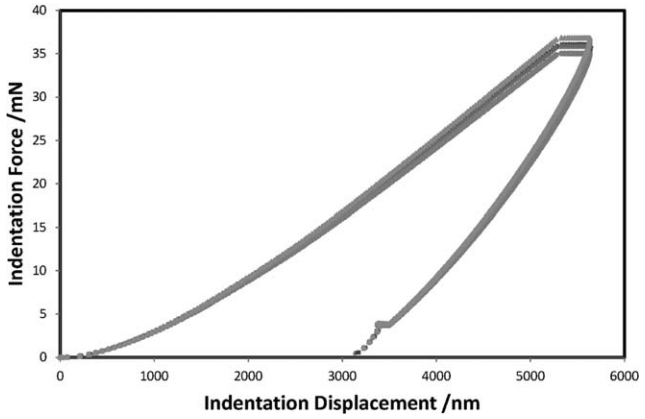

Figure 1. Indentation load–displacement data for the quenched PEEK sample at constant loading rate. The loading and unloading rates were maintained at 300 μN/sec. The loading portion was followed by a hold segment (20 sec) at the maximum indentation load.

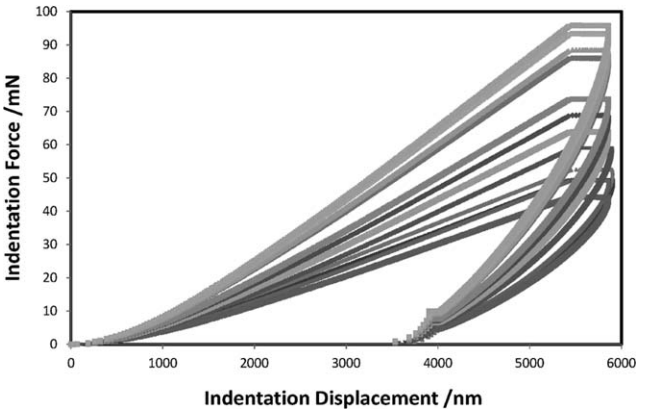

Figure 2. Indentation load–displacement data for the annealed (30% crystalline) PEEK sample at constant loading rate. The loading and unloading rates were maintained at 300 μN/sec. The loading portion was followed by a hold segment (20 sec) at the maximum indentation load.

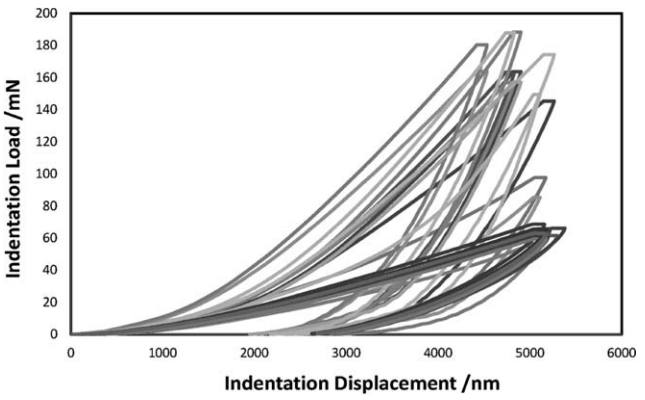

Figure 3. Indentation load–displacement data for the as received (40% crystalline) PEEK sample at constant loading rate. The loading and unloading rates were maintained at 300 μN/sec. The loading portion was followed by a hold segment (20 sec) at the maximum indentation load.

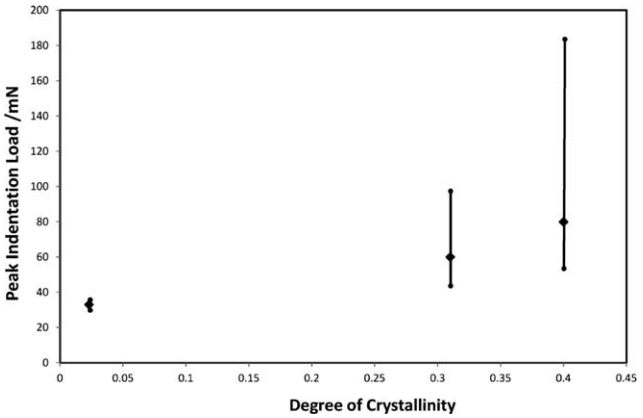

Figure 4. Peak indentation load, to induce 4000 nm penetration, as a function of degree of crystallinity of PEEK. The vertical lines embody range of peak indentation loads with mean of loads presented by rectangular pyramids.

reached at indentation force of 35 ± 2 mN. The plastic unrecoverable indentation depth at zero loads was 3100 ± 50 nm. Figure 2 is a typical loading–unloading cycle data set of the annealed (30% crystalline) PEEK. As can be seen from Figure 2, the maximum indentation displacement was achieved at different maximum loads 65 ± 30 mN. This bimodal peak behavior of the semicrystalline polymer is an indication of the multiphase present in the polymer. As can be seen from Figures 2 and 3, the indentation response of semicrystalline PEEK can be characterized as a multiphase response, similar to that of metal alloys.[22–25] The compliance data obtained from indentation of the virgin (40% crystalline) PEEK is presented in Figure 3. The multiphase behavior, multiple peak loads at the maximum indentation displacement, is prominent for the virgin semicrystalline polymer. The load–displacement curves can be grouped into two broad categories, a softer phase indentation in the region 50 ± 15 mN and a harder phase indentations 160 ± 20 mN at maximum penetration displacements. These multiphase responses were believed to be from the crystalline and amorphous regions of the polymer. The crystalline region was believed to be the one showing the harder response, whereas the amorphous regions were softer. The creep at maximum load hold segment was also found to be larger in amorphous regions compared to the harder crystalline domains. The indents in the intermediate regions were at places where the indentation depth was more than the thickness of crystalline lamellae. The polymeric surfaces were found to be harder in the increasing order of their degree of crystallinity of the polymer. The amorphous polymer is found to be softer, which required lower normal loads to induce comparable penetration depth.

Figure 4 shows the range of indentation peak loads observed to induce 4000 nm penetration depths in PEEK samples. As can be seen from Figure 4, the peak loads were within acceptable range of error (<5%) for the amorphous PEEK samples ($\approx$ 3% crystallinity). The range of observed peak values increase with increasing degree of crystallinity of the polymer. The large variations in the peak loads are an indication of the presence of multiplephases because of crystalline and amorphous regions in the semicrystalline polymer. The variations in the load–displacement data from indentation of the amorphous and the semicrystalline provides an initial insight for the presence of a bimodal behavior, which is confirmed later by the hardness and elastic modulus data as well.

Figure 5 shows the compliance curves of virgin (40% crystalline) PEEK at a constant effective strain rate of 0.025 sec^{-1}. The imposed rate of deformation during indentation, the strain rate $\dot{\varepsilon}$, is correlated with the displacement rate or the loading rate of the indenting body over the softer surface. In normal indentation, the strain rate acts in a direction perpendicular to the surface and may be defined as $\dot{\varepsilon} = k_2(\dot{h}/h)$, where h is the displacement, $\dot{h}$ is the nominal displacement rate and k_2 is a material constant, usually taken to be equal to 1.[6] Therefore, it may be defined as the inverse of the time required for the indenter to traverse a contact displacement unit. If the loading rate, $\dot{P}$, is the experimental parameter controlled during the indentation, the strain rate may be expressed as $\dot{\varepsilon} = k_2\left(\frac{\dot{P}}{h\left(\partial P/\partial h\right)}\right)$. The effective constant strain rates were achieved by applying constant displacement rate segments in terms of increasing displacements. These were selected as displacement rate of 1 nm/sec until 40 nm depth, then 2 nm/sec until 80 nm, 4 nm/sec till 160 nm, and so on to a displacement rate of 64 nm/sec to maximum depth of 2560 nm. A similar multiphase behavior as observed in constant loading rate segments was also observed in this type of experimentation. The ratio of peak loads for harder and softer phases of PEEK was found to be the major difference for constant loading rate segment and the constant strain rate indentation. The load–displacement data at constant loading rate has shown 3 : 1 harder to softer phase peak loads, whereas for constant strain rate experiments the ratio was observed to be 3 : 2. The difference in the experimental contact conditions may be the major reason for the different ratios. The effective strain rate is higher during initial loading for the constant loading rate segment; therefore, the peak depth has been achieved at lower normal loads for the softer region in the constant loading rate experiments compared to the constant strain experiments. The constant displacement

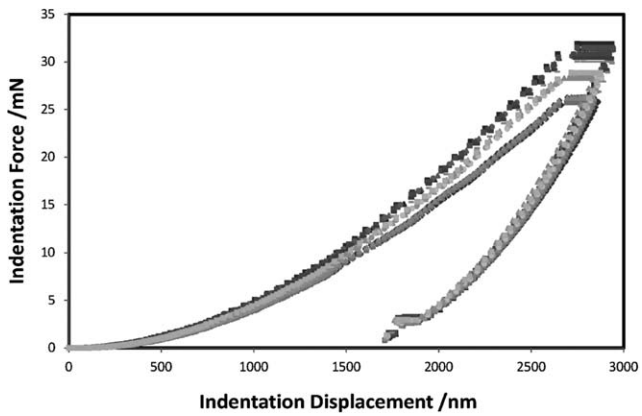

Figure 5. Indentation load–displacement data for the as received PEEK (40% crystalline) sample at constant strain rate. The effective strain rate was maintained at 0.025 sec^{-1} during loading segment.

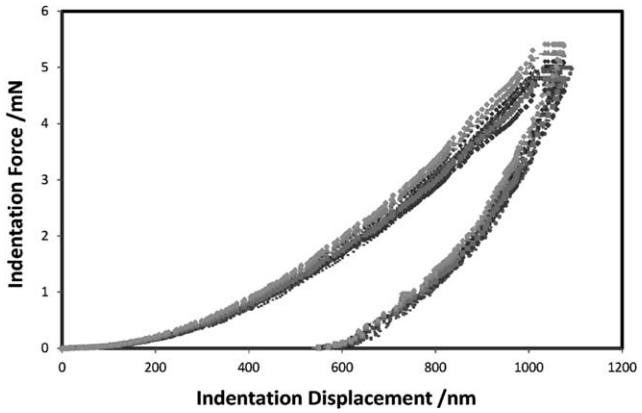

Figure 6. Indentation load–displacement data for the as received PEEK (40% crystalline) sample at constant strain rate. The displacement rate was maintained at 10 nm/sec during loading segment.

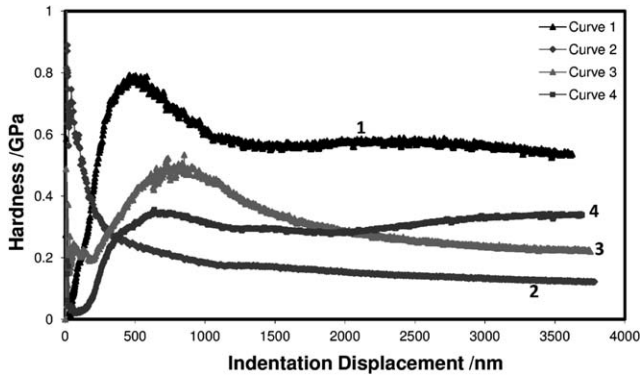

Figure 7. Indentation hardness as a function of indentation displacement data for the as received PEEK (40% crystalline) sample at constant loading rate of 300 μN/sec.

rate indentation load–displacement data are shown in Figure 6. Again multiphase behavior is evident from the curves and a ratio similar to the one observed in the constant strain rate experiments was seen. The bimodal character of the semicrystalline polymer is more prominent with increasing penetration depths.

Indentation Hardness and Elastic Modulus

Indentation Hardness. The normal indentation hardness data as a function of indentation depth for the virgin (40% crystalline) PEEK are presented in Figure 7. The figure shows only selected graphical data from the indentation experiments performed in different regions of the polymeric surface. The exceptional large variations were seen for hardness values at lower scales specifically at low penetration depths (<50 nm). These values were thought to be because of the errors present in surface determination, the tip geometry defects, and indentation size effects.[6,26,27] These values were not regarded as physically significant. A peculiar harder and more diverse response can be seen at near-to-surface layers particularly at penetration depth (100–500 nm) from all the figures. This can be attributed to localized modifications of the physical properties because of environmental exposure some time before the experiments or during the fabrication processing of polymeric materials. These near-to-surface modifications may have resulted from morphological aging or localized oxidation of the polymeric surfaces. It is interesting to note that the trends are similar in almost all cases. The observed near to surface hardness response is similar to the one reported by Briscoe and co-workers.[6] They have reported large uncertainties in the hardness of polymers for different polymeric systems with nanoindentation without the application of the continuous stiffness mode.

Therefore the hardness values corresponding to indentation depths of more than 500 nm will be considered mainly for the property evaluations. The multiphase behavior, as depicted earlier from the load–displacement compliance curves of PEEK, can be confirmed from these hardness-depth graphs. The diverse multiphase response of PEEK can be interpreted from Figure 7. Curve 2 in the figure corresponds to the softer phase with hardness of approximately 0.2 GPa and curve 1 indicating the harder phase present in the polymeric material with 0.55 GPa indentation hardness. The curves 3 and 4 characterize the indentation through multiphase regions that is harder and softer regions of the polymers. An interesting fact can be noted from the two curves that they were either harder or softer initially and then switch the properties at approximately 2000 nm. As can be seen in the figure curve 3 shows a harder region of the polymeric surface at lower penetration depths and then a continuous decreasing trend of the hardness at higher penetration indicating softer regions underneath. In comparison, the curve 4 shows a softer region initially while harder one at higher penetration depths. There are no comparable data on bimodal character of semicrystalline polymers in the literature. The bimodal indentation response of metal alloys is reported in terms of hard and soft phases.[23,25,26]

The indentation hardness as a function of penetration depth for the quenched (amorphous), the annealed, and the virgin semicrystalline PEEK surfaces are presented in Figure 8. The hardness data presented are based on the median of the compliance curves for the respective polymeric surfaces only for comparative purposes. A peculiar surface hardening of the polymeric surfaces was observed for all the polymers. Comparatively

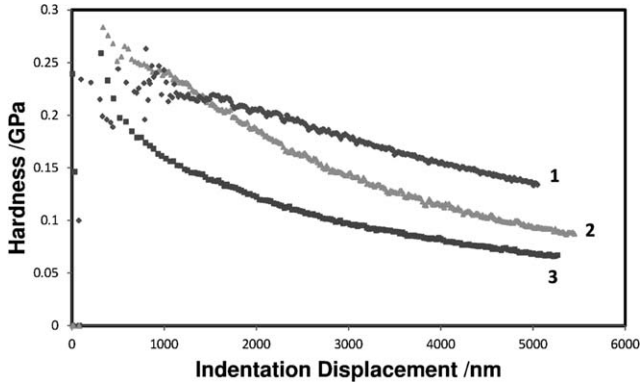

Figure 8. Hardness as a function of indentation displacement data for the quenched PEEK (curve 3), the annealed PEEK (curve 2) and the virgin PEEK (curve 1) sample at constant loading rate of 300 μN/sec. The hardness is averaged from a minimum of 25 indentation experiments for each polymer.

Applied Polymer SCIENCE

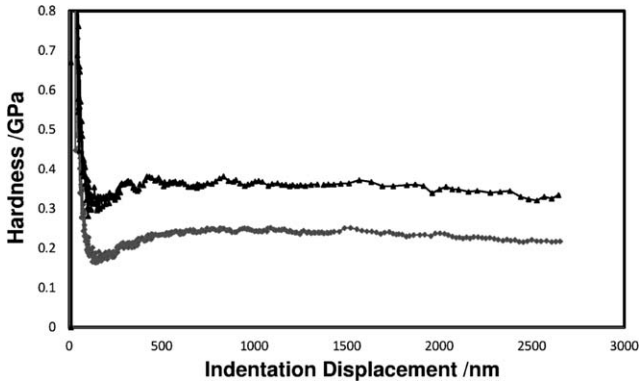

Figure 9. Indentation hardness as a function of indentation displacement data for the as received PEEK sample at constant strain rate of 0.025 sec^{-1}.

higher gradients in the surface hardening response were seen for the thermally treated polymers as compared to the virgin semicrystalline polymers. These higher surface hardening gradients can be attributed to the thermal treatment history of the polymers. The induction phase, lower indentation displacement, hardness values originated from the tip calibration defects at lower penetration depths can be neglected. An increasing trend of the measured hardness was observed with the increase of the crystallinity of the PEEK surfaces. The calculated hardness values for the amorphous PEEK were similar to the ones reported by Deslandes and Rosa.[27] They have established an interrelationship between the crystallinity of PEEK and the microhardness. Although the trends in increasing crystallinity were similar, comparatively lower hardness values were observed in the present study in comparison to those given by Deslands and Rosa[27] for crystalline PEEK surfaces (255 ± 20 MPa). These differences in the computed hardness values can be attributed to the indentation scale effects and the differing experimental procedures. They have performed the experiment using Buehler Micromet II microhardness tester equipped with a diamond square pyramid tip of included angle 136° under a load of 100 g for 5 sec. The hardness was then evaluated by determining the indentation area by an imaging technique.

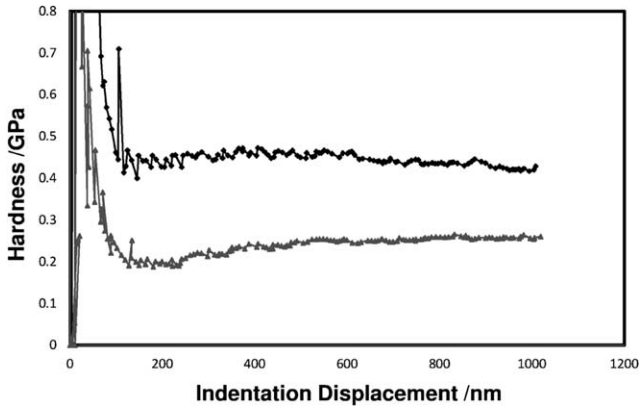

Figure 10. Indentation hardness as a function of indentation displacement data for the as received PEEK sample at constant displacement rate of 10 nm/sec.

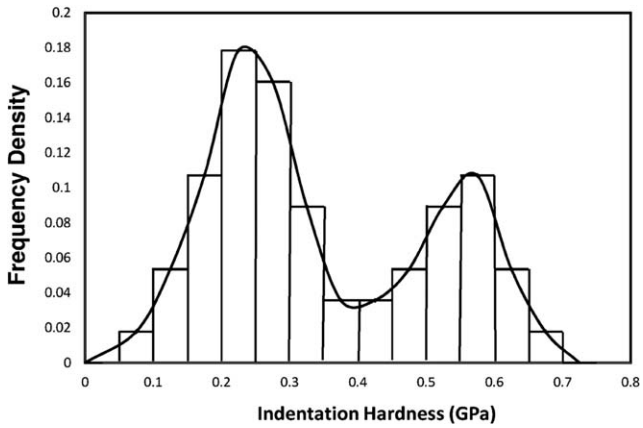

Figure 11. Frequency density distribution based on Indentation hardness of semicrystalline PEEK sample. The frequency is calculated on a sample width of 0.05 GPa and based on 50 indents at constant loading rate of 300 μN/sec.

Figures 9 and 10 present the selected hardness data of the virgin semicrystalline PEEK obtained at the constant strain rate and the constant displacement rate loadings, respectively. The figures provided further evidence for the bimodal response of the semicrystalline PEEK during indentation. The indentation hardness as a function of displacement is shown in these figures under constant strain rate and displacement loadings, respectively. As can be seen from the figures a strain softening response for the harder phase and a strain hardening response for the softer phase is also evident.

Frequency Distribution. The indentation hardness frequency density distribution, based on a sample length of 0.05 GPa in the interpolated data from 50 indents is presented in Figure 11. The hardness values were taken at 4000 nm for each indent. The presence of two peaks in the distribution clearly indicates the bimodal nature of the polymer. The first peak at approximately 0.2 GPa corresponds to the softer amorphous phase of the polymer. The harder crystalline phase had given rise to the second peak at about 0.55 GPa. Therefore, 0.2 GPa is found to be the limiting hardness difference differentiating the amorphous and the crystalline phases. The bimodal character will disappear if a larger step size for the frequency distribution is

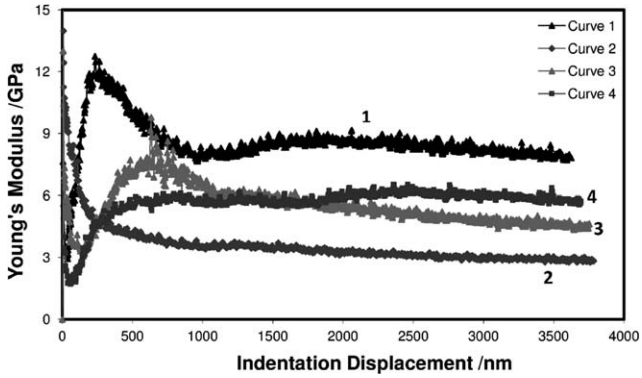

Figure 12. Elastic Young's Modulus as a function of indentation displacement data for the as received semicrystalline PEEK sample at constant loading rateof 300 μN/sec.

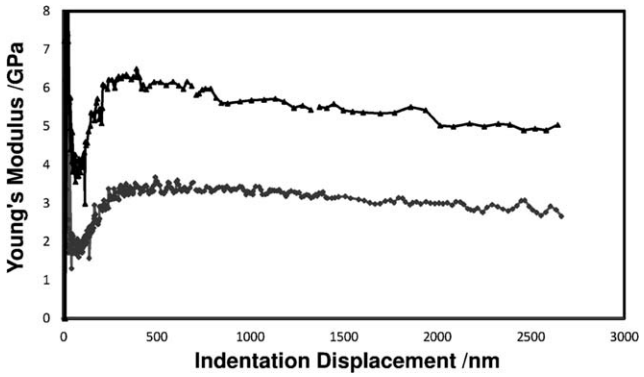

Figure 13. Elastic Young's Modulus as a function of indentation displacement data for the as received semicrystalline PEEK sample at constant strain rate of 0.025 sec^{-1}.

selected. The differences in hardness of an amorphous and a crystalline phase of a semicrystalline polymer can be because of the differences in the chain mobility and the density differences. The crystalline portion was estimated to be 36% on the basis of a peak area, which is similar to the crystallinity of the polymer as estimated by the DSC analysis. The peak area was calculated from the height of the histogram columns. Hence, the nanoindentation hardness provides a convenient and a nondestructive method for the degree of crystallinity determination of a semicrystalline polymer.

Young's Modulus. The elastic modulus of semicrystalline PEEK as a function of indentation displacement is shown in Figures 12–14 for different loading conditions. These curves also conform to the presence of multiphases in the semicrystalline polymer as discussed above with indentation hardness. The hard crystalline phase is estimated to have a modulus of 8 GPa (curve 1) and the amorphous soft phase approximately 4 GPa (curve 2). Similar results were seen for elastic modulus values from indentation experiments performed under a constant strain rate and constant displacement rate. As can be seen from Figures 13 and 14, the two curves are smoother in the softer phase, whereas there were higher fluctuations present in the harder crystalline phases. These fluctuations might be because of higher plastic deformations taking place in the hard phase.

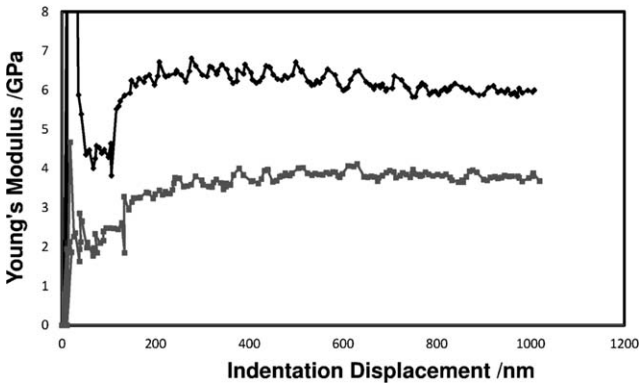

Figure 14. Elastic Young's Modulus as a function of indentation displacement data for the as received semicrystalline PEEK sample at constant displacement rate of 10 nm/sec.

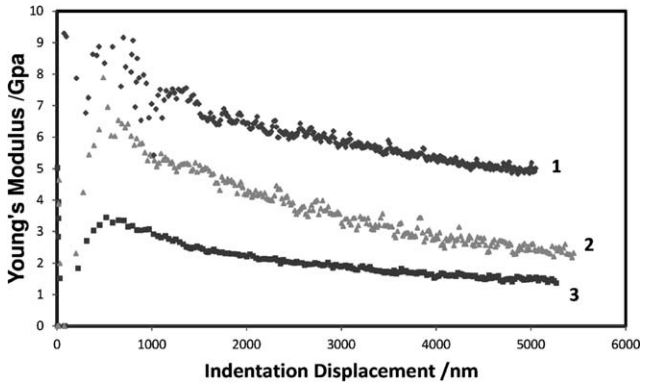

Figure 15. Elastic Young's Modulus as a function of indentation displacement data for the quenched PEEK (curve 3), the annealed PEEK (curve 2), and the virgin PEEK (curve 1) sample at constant loading rate of 300 μN/sec.

Another reason might be the indentation depth has exceeded the crystal size of this phase thus entering the amorphous and the crystalline phase boundaries.

Figure 15 shows the elastic Young's Modulus data of the PEEK surfaces as a function of indentation contact displacement, computed using the continuous stiffness method. Young's Modulus was evaluated using a modulus of 1141 GPa and a Poisson's Ratio of 0.07 for the diamond indenter.[28] The figure shows a strong increasing trend for the modulus values with the decreasing of the indentation depth for all the systems. These trends are similar to those observed for the normal hardness (Figure 15). The possible localized minor modification or surface crystallinity of the material properties of the near-to-surface layers of the PEEK during fabrication could provide an acceptable explanation for the higher modulus value near to the surface as compared to the bulk values. The elastic modulus was found to be increasing with the increasing of the crystallinity of the polymer. The fact that the modulus curves for the semicrystalline polymers were significantly noisier than the amorphous polymers especially at lower penetration depths is probably because of complex discontinuous deformation processes during indentation into the semicrystalline polymers.

Periodicity in Properties. The periodic nature of the fluctuations observed in the nanoindentation data was analyzed by correlation analysis for the presence of any regularity or periodicity. The experimental data were used to obtain a polynomial function in the range with minimum experimental errors, i.e., 2000–3000 nm indentation displacement. The overall trends of the data were then removed to observe the periodicity or regularity. Figures 16–18 present some selected data showing the fluctuations, after removal of the established trend from the experimental data for the elastic modulus of the quenched, the annealed and the virgin PEEK (the data points are linked for the sake of clarity). As can be seen from Figure 16 the data are reasonably smooth for the quenched PEEK. Periodic fluctuations in properties of the semicrystalline polymers were observed as can be seen in Figures 17 and 18. These fluctuations appear to be governed by discontinuities in the polymeric materials and can be related to the spherulites present in the

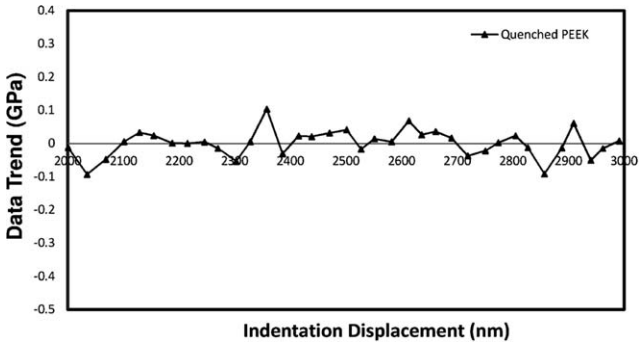

Figure 16. Data trend based on removal of the main trend for the elastic modulus of quenched PEEK as a function of indentation displacement data in the range 2000 nm to 3000 nm.

semicrystalline PEEK. The period (≈200 nm) of these fluctuations corresponds to the likely size of mesophase. The spherulite sizes of the PEEK in case of crystallization across carbon fiber composites were reported to be 10–20 μm.[29] Therefore it might correspond to the thickness of mesophase of the crystals in the polymer.[30] A clear morphological description of the semicrystalline PEEK is not available without extensive and costly investigation. This might include X-ray, transmission electron microscope, and neutron scattering although precedents have not been clearly established.

Therefore, the bimodal character of the semicrystalline polymers is established from the continuous stiffness mode indentation. The reported surface mechanical properties are shown to be influenced by the degree of crystallinity of the polymer. The bimodal character may not be observed from the conventional macroindentation data because of averaging of the data from all the indents. The conventional indentations provide single point data from each indent evaluated at the maximum loading point. The data obtained from different indents are averaged to elucidate the hardness and the elastic modulus of the surfaces. As shown above, the bimodal character of the semicrystalline polymers can only be obtained from the continuous hardness and the elastic modulus data evaluations as function of the imposed displacement as well as by the selection of a proper sample length for the frequency density and time series analysis of the data.

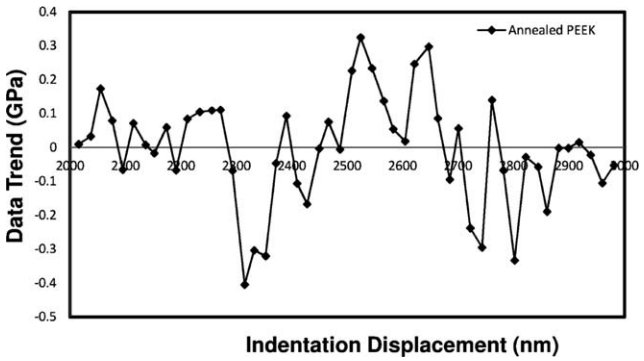

Figure 17. Data trend based on removal of the main trend for the elastic modulus of annealed PEEK as a function of indentation displacement data in the range 2000–3000 nm.

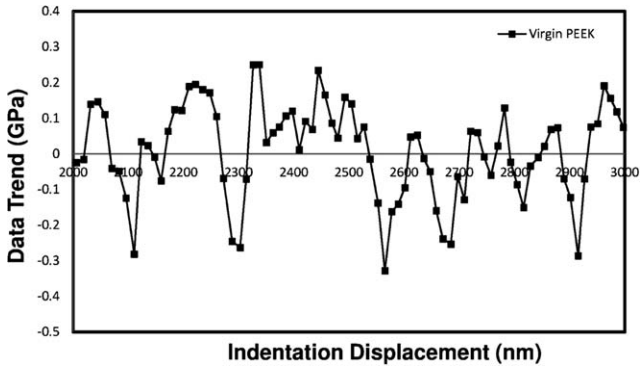

Figure 18. Data trend based on removal of the main trend for the elastic modulus of the as received (virgin) semicrystalline PEEK as a function of indentation displacement data in the range 2000–3000 nm.

CONCLUSION

This article presents the experimental results from normal indentations performed on amorphous and semicrystalline PEEK at depths of 0–5 μm. The surface mechanical properties were seen to be influenced by the indenter loading conditions and the penetration displacements utilized. Data for the elastic modulus and the hardness are presented for all polymeric materials and are found to be dependent on contact conditions. These properties appear to be unreliable at penetration displacements close to the surface. This can be because of change in the mechanical and physical properties of polymers because of their manufacture or aging. However, the most probable reason might be the precise unestablished imperfections in the indenter tip calibration. The surface mechanical properties of the semicrystalline polymers are a function of the degree of crystallinity. The higher the crystalline content of the polymer, more will be the ordering of the molecular chains. Hence the greater are the surface mechanical properties of the polymeric surface. A bimodal response to indentation is observed for semicrystalline polymer. A method to calculate the crystallinity of the semicrystalline polymers based on nondestructive indentation has been developed. The bimodal character is confirmed by the load–displacement, the hardness, and the elastic modulus data. The creep at maximum load hold segment was also found to be larger in amorphous regions compared to the harder crystalline domains. The bimodal response was thought to depend upon whether the polymer is indented in the softer, amorphous phase or the harder, crystalline phase. The proportion of the two regions was found to be similar to the ratio of crystallinity of the polymer. The precise mode of bimodal character depends upon the selection of a proper data interpolation that is sample length for the time series analysis of the data. Periodic fluctuations in the surface mechanical properties of the semicrystalline polymers were found with increasing penetration depths. These fluctuations were likely to arise from the material heterogeneities, namely crystalline spherulites in the semicrystalline polymers. Morphological investigations of the semicrystalline polymers would further elucidate these fluctuations.

Finally, the continuous stiffness mode nanoindentation method is found to be a convenient method for investigating surface mechanical properties of semicrystalline polymers, which show

bimodal and viscoelastic-plastic behavior. The nanoindentation technique may provide a convenient means to understand morphological description of the polymeric surfaces.

ACKNOWLEDGMENTS

The authors would like to thank Mr. D. Parsonage, Chemical Engineering & Technology Department, Imperial College, London, for his help with nanoindenter calibration.

REFERENCES

1. Oliver, W. C.; Pharr, G. M. *J. Mater. Res.* **1992**, *7*, 1564.
2. Briscoe, B. J.; Sebastian, S. K. *Proc. R. Soc. A Math. Phys. Eng. Sci.* **1996**, *452*, 439.
3. Doerner, M. F.; Nix, W. D. *J. Mater. Res.* **1986**, *1*, 601.
4. Loubet, J. L.; Georges, J. M.; Marchesini, O.; Meille, G. *J. Tribol.* **1984**, *106*, 43.
5. Brostow, W.; Kovačević, V.; Vrsaljko, D.; Whitworth, J. *J. Mater. Edu.*, **2010**, *32*, 273.
6. Briscoe,B. J.; Fiori, L.; Pelillo, E. *J. Phys.D Appl. Phys.*, **1987**, *31*, 2395.
7. Iqbal, T.; Briscoe, B. J.; Luckham, P. F. *Eur. Polym. J.* **2011**,*47*, 2244–2258.
8. Li, X.; Bhushan, B. *Mater. Charact.* **2002**, *48*, 11.
9. Oliver, W. C.; Pharr, G. M. *J. Mater. Res.* **2004**, *19*, 3.
10. Jiang, W. G.; Su, J. J.; Feng, X. Q. *Eng. Fract. Mech.*, **2008**, *75*, 4965.
11. Babu, J. S. S.; Kang, C. G. *Mater. Des.* **2010**, *31*, 4881.
12. Page, T. F.; Pharr, G. M.; Hay, J. C.; Oliver, W. C.; Lucas, B. N.; Herbert, E.; Riester, L. *In Mater. Res. Soc. Symp. Proc.* **1998**.
13. Tze, W. T. Y.; Wang, S.; Rials, T. G.; Pharr, G. M.; Kelley, S. S. *Compos. Appl. Sci. Manuf.* **2007**, *38*, 945.
14. Ion, R. H.; Pollock, H. M.; Roques-Carmes, C. *J. Mater. Sci.*, **1990**, *25*, 1444.
15. Briscoe, B. J.; Sebastian, K. S.; Sinha, S. K. *Philos. Mag. A* **1996**, *74*, 1159.
16. Chu, J.; Kamal, M. R.; Derdouri, S.; Hrymak. A. In *Technical Papers, Regional Technical Conference-Society of Plastics Engineers.* **2008**.
17. Rose, J. B. Aromatic polymers containing ketone linking groups and process for their preparation. *Brit. Pat.* **1975** (3928295).
18. Xing, P.; Robertson, G. P.; Guiver, M. D.; Mikhailenko, S. D.; Kaliaguine, S. *Macromolecules* **2004**, *37*, 7960.
19. Pethica, J. B.; Oliver, W. C. *MRS Symp. Proc. Mater. Res. Soc.* **1989**, *130*, 13.
20. Lucas, B. N.; Oliver, W. C.; Swindeman, J. E. In Materials Research Society Symposium—Proceedings, **1998**.
21. Naffakh, M.; Gomez, M. A.; Ellis, G.; Marco, C. *Polym. Eng. Sci.* **2006**, *46*, 1411.
22. Chen, C. L.; Richter, A.; Thomson, R. C. *Intermetallics* **2009**, *18*, 499.
23. Gerday, A. F.; Bettaieb, M. B.; Duchene, L.; Clement, N.; Diarra, H.; Habraken, A. M. *Acta Mater.* **2009**, *57*, 5186.
24. Chen, J. J.; Sorelli, L.; Vandamme, M.; Ulm, F. J.; Chanvillard, G. *J. Am. Ceram. Soc.* **2010**, *93*, 1484.
25. Xia, S.;Wang, W. *J. Mater. Trans.* **2010**, *51*, 36.
26. Bonne, M.; Briscoe, B. J.; Lawrence, C. J.; Manimaaran, S.; Parsonage, D.; Allan, A. *Tribol. Lett.* **2005**, *18*, 125.
27. Deslandes, Y.; Rosa, E. A. *Polym. Commun.* **1990**, *31*, 269.
28. Klein, C. *Mater. Res. Bull.* **1992**, *27*, 1407.
29. Wang, W.; Qi, Z.; Jeronimidis, G. *J. Mater. Sci.* **1991**, *26*, 5915.
30. Singh, S.; Dunmur, D. A. Liquid Crystals: Fundamentals; World Scientific Publishing: London, **2002**.